



HAL
open science

Polyp longevity in a precious gorgonian coral: hints toward a demographic approach to polyp dynamics

Maria Carla Benedetti, Lorenzo Bramanti, Cristina Priori, Fabrizio Erra, Mimmo Iannelli, Fabio Bulleri, Giovanni Santangelo

► To cite this version:

Maria Carla Benedetti, Lorenzo Bramanti, Cristina Priori, Fabrizio Erra, Mimmo Iannelli, et al.. Polyp longevity in a precious gorgonian coral: hints toward a demographic approach to polyp dynamics. Coral Reefs, 2020, 39 (4), pp.1125-1136. 10.1007/s00338-020-01942-6 . hal-02927645

HAL Id: hal-02927645

<https://hal.sorbonne-universite.fr/hal-02927645v1>

Submitted on 24 Nov 2020

HAL is a multi-disciplinary open access archive for the deposit and dissemination of scientific research documents, whether they are published or not. The documents may come from teaching and research institutions in France or abroad, or from public or private research centers.

L'archive ouverte pluridisciplinaire **HAL**, est destinée au dépôt et à la diffusion de documents scientifiques de niveau recherche, publiés ou non, émanant des établissements d'enseignement et de recherche français ou étrangers, des laboratoires publics ou privés.



1 REPORT

2 **Polyp longevity in a precious gorgonian coral: hints toward**
3 **a demographic approach to polyp dynamics**

4 **Maria Carla Benedetti**¹ · **Lorenzo Bramanti**² · **Cristina Priori**¹ · **Fabrizio Erra**¹ ·
5 **Mimmo Iannelli**³ · **Fabio Bulleri**¹ · **Giovanni Santangelo**¹

6 Received: 12 December 2018 / Accepted: 24 April 2020
7 © Springer-Verlag GmbH Germany, part of Springer Nature 2020

8 **Abstract** In this paper, we investigated the age distribu-
9 tion and dynamics of polyps in the slow-growing and long-
10 lived gorgonian *Corallium rubrum* (the Mediterranean red
11 coral), applying an a posteriori demographic approach by
12 considering each colony as a population of polyps. In the
13 Mediterranean red coral, new polyps emerge from the
14 coenenchyme in different regions of the colony and their
15 budding rate depends on the age of branches. The age of
16 polyps, branches and colonies were estimated using the
17 organic-matter-staining dating method on thin sections of
18 the colony skeleton. The median age and maximum life
19 span of polyps were 4 and 12 years suggesting the presence
20 of senescence processes: thus a colony renews several
21 times its polyps during life cycle. Polyps were divided into
22 annual age classes, and their mortality rates calculated. The
23 polyp age distribution was then used to construct a mor-
24 tality table and an algebraic transition matrix based on the
25 age at death of 234 polyps. Finally, the polyp budding rate
26 of a young, unbranched colony was calculated, and polyp
27 temporal dynamics simulated. These findings represent the

first steps for developing demographic models able to 28
describe polyp dynamics of old and highly branched 29
colonies. 30

Keywords Octocoral · Polyp age · Mortality table · 32
Budding rate 33

Introduction 34

Modularity is a common feature among plants and inver- 35
tebrates. Nowadays, the term modular is mainly used as 36
synonymous of hierarchical and refers to the repetition of 37
homogenous units at different organization levels (Rosen 38
1986; Kim and Lasker 1998; Hageman 2003). The first 39
definition of corals as modular organisms can be found in 40
Harper (1977). Polyps, embedded in the coenenchyme, are 41
the primary modules of colonial corals. They are the basic 42
units of a colony, likely determining its shape by regulating 43
the growth of branches (second-order modules, called 44
structural units, Hageman et al. 1998; Hageman 2003). 45
Therefore, the fundamental body plan of a colonial coral, 46
often characterized by different growth forms, results from 47
the repetition of units, *i.e.* polyps and branches of several 48
orders and varying lengths (Williams 1975; Harper 1977; 49
Harper and Bell 1979; Burlando et al. 1991; Lasker et al. 50
2003; Sánchez and Lasker 2003; Sánchez et al. 2004; 51
Goffredo and Lasker 2006). 52

Morphological plasticity, typical of modular organisms, 53
is likely the result of genotypic variability or phenotypic 54
response to local environmental conditions (*e.g.*, Shaish 55
et al. 2006, 2007; Sánchez et al. 2007; Rowley et al. 2015; 56
Guizien and Ghisalberti 2017). The optimal shape of a 57
stony-coral colony is the result of the polyp ability to 58
calcify (Matsumoto 2004; Goffredo and Lasker 2006) and 59

A1 Topic Editor Andrew Hoey

A2 **Electronic supplementary material** The online version of this
A3 article (<https://doi.org/10.1007/s00338-020-01942-6>) contains sup-
A4plementary material, which is available to authorized users.

A5 Maria Carla Benedetti
A6 carlottabenedetti88@hotmail.it

A7 ¹ Department of Biology, University of Pisa, CoNISMa, Via
A8 Volta 6, 56126 Pisa, Italy

A9 ² Sorbonne Université, CNRS, Laboratoire d'Ecogéochimie
A10 des Environnements Benthiques, LECOB,
A11 66650 Banyuls-sur-Mer, France

A12 ³ Department of Mathematics, University of Trento, Via
A13 Sommarive 14, 38123 Povo, TN, Italy

60 can thus be affected by polyp distribution and density
61 (Rossi et al. 2019). For example, ramified gorgonians have
62 evolved a prey capture structure by which barbed tentacles
63 of polyps and branches form an efficient fishing net inter-
64 cepting water flow thus feeding on detrital particulate
65 organic matter (POM) and microplankton (Barham and
66 Davies 1968; Grigg 1972; Russo 1985; Coma et al. 2001;
67 Kaandorp and Küler 2001; Tsounis et al. 2006b; Picciano
68 and Ferrier-Pagès 2007; Pedoni et al. 2009; Gori et al.
69 2011).

70 Merks et al. (2004) described coral growth as the
71 “collective result of a growth process taking place in the
72 polyps.” In their “polyp-oriented model,” polyps are
73 considered as separate units, which during their life cycle
74 deposit skeleton, bud new polyps and eventually die. Each
75 colony can then be considered as a population of polyps
76 and branches (belonging to the same genet; Harper 1977;
77 Galli et al. 2016); thus, its growth over time can be pro-
78 jected by dynamic models based on polyp growth and
79 mortality rates, as well as increase in branch number.
80 Under these circumstances, integrating data from individ-
81 ual and modular growth studies may enhance the under-
82 standing of growth in highly plastic corals. Precious corals
83 belonging to the Family Corallidae are generally slow-
84 growing and long-lived, thus, following their growth over
85 the entire life span is a nearly impossible task (Santangelo
86 et al. 2003) and indirect methods to assess colony devel-
87 opment in these species are needed (Marschal et al. 2004;
88 Vielzeuf et al. 2008; Benedetti et al. 2016; Kahra-
89 manoğullari et al. 2019).

90 We investigated polyp formation, age and spatial dis-
91 tribution in the highly valuable octocoral *Corallium*
92 *rubrum* (L 1758; Fig. 1), considering the iteration of the
93 primary modules (polyps) as the lowest level of colony
94 organization. *C. rubrum* is a long-lived Mediterranean
95 gorgonian, whose life span can exceed a century (Marschal
96 et al. 2004; Priori et al. 2013). This species is endemic to
97 the Mediterranean Sea and neighboring Atlantic rocky
98 bottoms, where it dwells between 10 and 1000 m depth.
99 Within this wide bathymetric distribution, shallow
100 (< 50 m), deep (50–200 m), and deeper populations
101 (> 200 m) have been conventionally distinguished by an
102 operative point of view (Santangelo and Abbiati 2001;
103 Costantini et al. 2011; Knittweis et al. 2016). *C. rubrum*
104 has long been subjected to commercial fishing, as its red
105 calcareous skeleton is widely used in jewelry and traded
106 worldwide (e.g., Cicogna and Cattaneo-Vietti 1993;
107 Tsounis et al. 2010). Due to its slow growth rates
108 ($\sim 0.24 \text{ mm y}^{-1}$ in basal diameter; Marschal et al. 2004;
109 Priori et al. 2013; Bramanti et al. 2014; Benedetti et al.
110 2016), the overharvesting of larger/older colonies has
111 caused an alarming shift in the structure of existing pop-
112 ulations toward smaller sizes (Santangelo and Abbiati

2001; Tsounis et al. 2006a; Bramanti et al. 2009; Cau et al. 113
2016; Garrabou et al. 2017). *C. rubrum* has therefore been 114
included in three different international conventions (EU 115
Directive Habitat, Bern Convention, and Convention on 116
Biological Diversity) and its harvesting is regulated by 117
Mediterranean, national and local/regional rules (GFCM- 118
FAO 2011). For species with long life span and complex 119
life cycle such as *C. rubrum* demographic studies are 120
required to advise policy makers on the most appropriate 121
conservation and management strategies (Santangelo et al. 122
2007; Bramanti et al. 2009). 123

124 A first step to assess population demographic dynamics
125 is estimating the age of its components (Bramanti et al. 125
2017). Age distribution data can be used for developing 126
life history tables and for projecting population trends 127
over time by means of algebraic transition matrices 128
(Caswell 2001; Fujiwara and Caswell 2001; Santangelo 129
et al. 2015). 130

131 In this paper, we scale this approach down from the
132 population to the colony level, considering a single col-
133 ony as a population of polyps. While several studies have
134 dealt with aging in octocorals (e.g., Sherwood 2006;
135 Thresher et al. 2009), little is known about the aging and
136 life span of polyps. We applied a novel method for
137 assessing the age of Mediterranean red coral polyps
138 (Vielzeuf et al. 2008) and their turnover to build a life
139 history table (mortality table). In order to estimate the
140 budding rate of polyps in a young colony and to project
141 its structure through time, a transition matrix of polyp
142 survival was constructed by means life history data. Thus,
143 our work focuses on: (1) early skeleton formation and
144 dynamics of polyp number, (2) distribution of polyp age
145 and density across the colony, (3) polyp life span, mor-
146 tality and variations in budding rate through time.

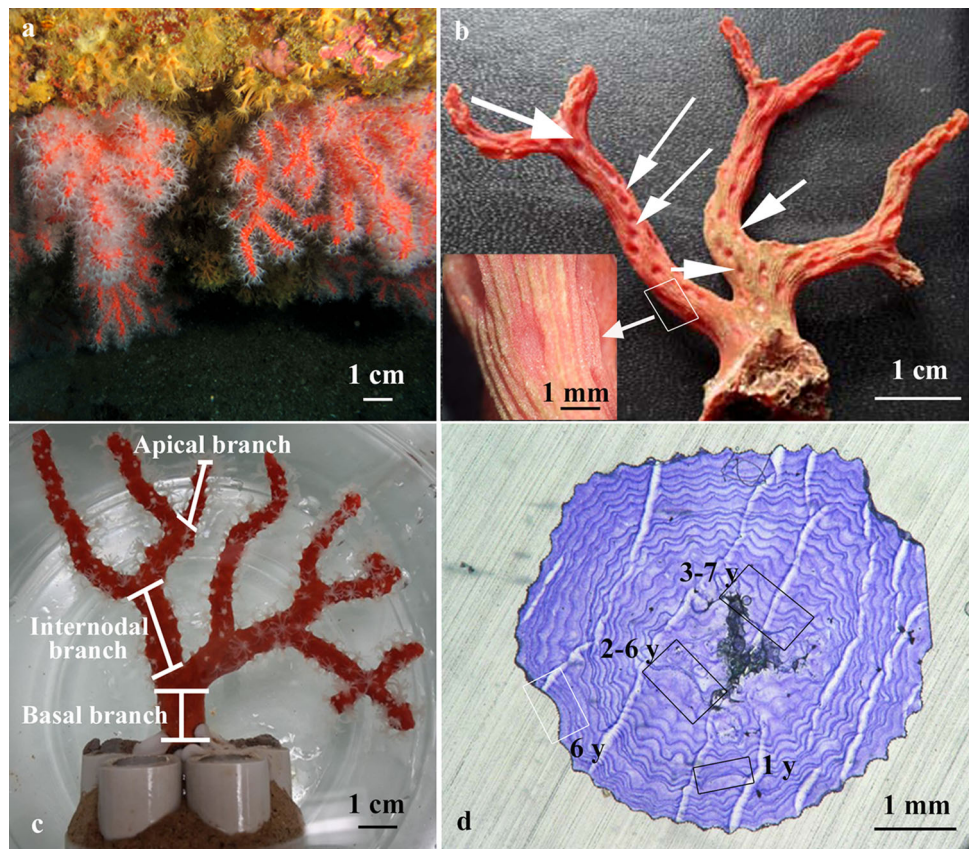
147 Materials and methods

148 *C. rubrum* basic features

149 The Mediterranean red coral is gonochoric at both the
150 polyp and colony levels and is characterized by a long life
151 span and an early age at first reproduction (Santangelo
152 et al. 2003; Gallmetzer et al. 2010). It is an internal brooder
153 whose larvae are released yearly in late summer and settle
154 within 20–25 days (L Bramanti personal observ.). After
155 settlement, metamorphosis occurs in approximately
156 10 days (L Bramanti pers. observ.) and a new colony starts
157 growing (Lacaze Duthiers 1864; Vighi 1972).

158 Similarly to other colonial octocorals, *C. rubrum* has
159 polyps embedded in the coenenchyme, and their gas-
160 trovascular cavities are interconnected by superficial and
161 deep gastrodermal channels (Lacaze Duthiers 1864). The

Fig. 1 **a** *Corallium rubrum* colonies in the Marine Protected Area of Cerbere/Banyuls sur Mer (L Bramanti photorecredits); **b** A colony depleted of coenenchyme (arrows indicate polyp cavity marks) and a detail of crenulated colony axis with a polyp cavity mark without crenulations. **c** Three types of branches in a *C. rubrum* colony; **d** Thin OMS section of colony axis where annual growth rings are highlighted. Three dead (black rectangles) and one living polyp cavity mark (white rectangle) are shown



162 superficial channels are small and located within the coenenchyme layer, while the deep channels are larger and located in crenulations (wavelets) along the skeleton surface. When the coenenchyme and polyps are removed, a cavity mark can be distinguished, imprinted on the skeleton just below the polyp (Fig. 1b; Lacaze Duthiers 1864; Grillo et al. 1993; Vielzeuf et al. 2008). The deep channels are absent on the surface of these cavity marks, hence no crenulations are found below the polyps (Fig. 1b; Perrin et al. 2015).

172 Skeleton formation and dynamics of polyp number

173 The early skeleton formation in 1–4-year-old colonies (settled on artificial substrates; see Bramanti et al. 2005, 2007) has been examined under a dissection microscope (40–60 x; Fig. 2).

177 The relationship between total number of polyps and branches was tested on 518 intact colonies of different size (out of 695 collected across the Northwestern Mediterranean between 2009 and 2016; Priori et al. 2013; Bramanti et al. 2014; Benedetti et al. 2016; unfortunately no environmental data on sampling sites was at our disposal (sampling details in Supplemental Materials). All the colonies were photographed, numbered and fixed in 4% formalin for laboratory analysis. The total number of

186 polyps and the sex of each colony were determined under a binocular dissecting microscope (Santangelo et al. 2003).

187
188 Three types of branches were identified in each colony: basal, internodal and apical. The basal branch corresponds to the base of the colony, the internodal branch is the first branch generated by the branching process (i.e., the largest/oldest branch of the colony; Benedetti et al. 2016) and the apical branch was chosen randomly among the tips (Fig. 1c).

195 The relationship between the number of apical branches and the number of polyps was assessed by means of linear, power, logarithmic and exponential fits and the one with the highest R^2 was selected. Significance was tested by Pearson's correlation coefficient on log/log transformed data.

201 Polyp age and distribution

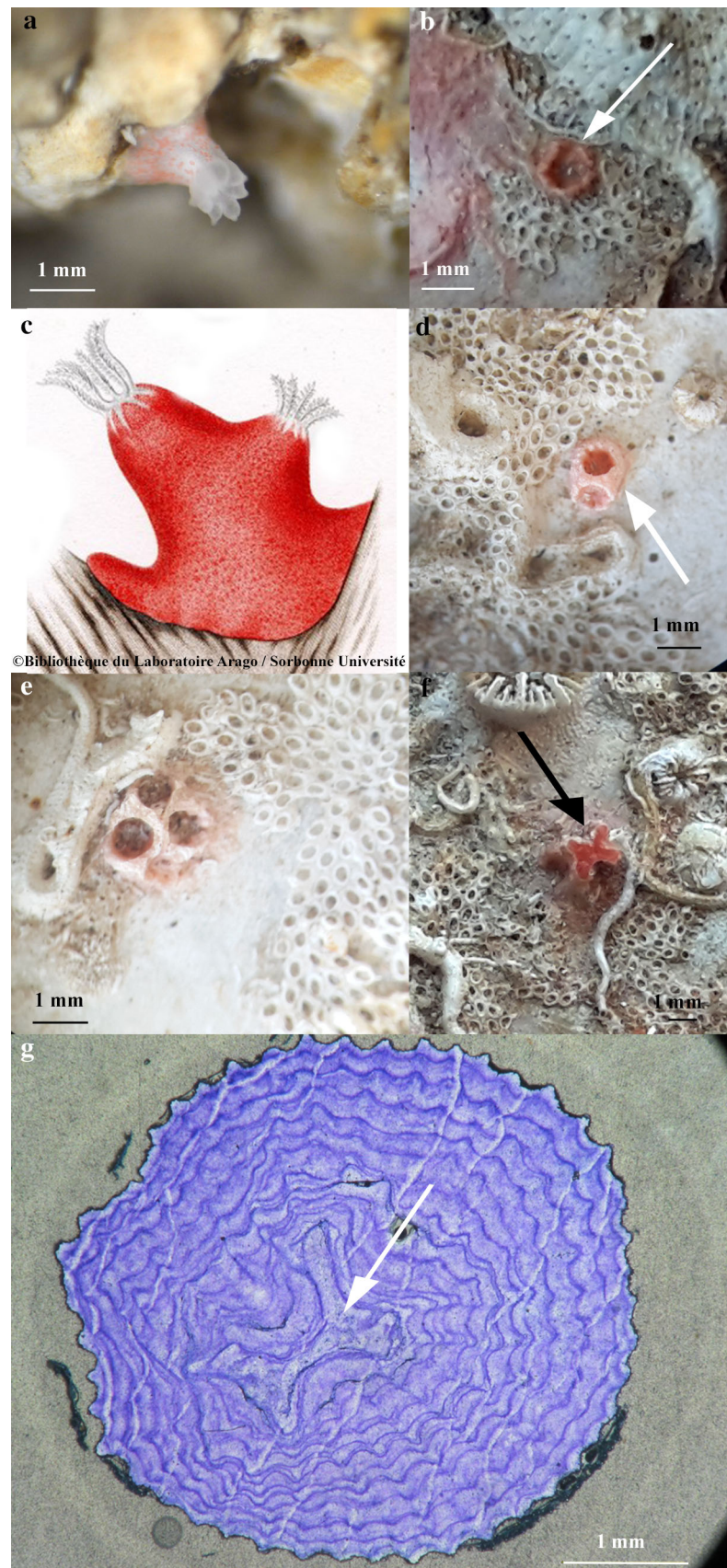
202 The age of polyps was estimated by applying the procedure developed by Vielzeuf et al. (2008) based on the Organic Matrix Staining (OMS) method for colony dating (Marchal et al. 2004), which highlights annual growth rings on decalcified and stained thin sections (50 μ m), transversal to colony axis. Only 135 colonies (out of 695) were suitable for this analysis (i.e., without signs of damage by boring sponges). Overall, 197 transverse thin sections cut

186
187
188
189
190
191
192
193
194
195
196
197
198
199
200

201

202
203
204
205
206
207
208
209

Fig. 2 Formation of *C. rubrum* skeleton starting from the walls of cavity marks: **a** Young colony at 1 polyp-stage (L Bramanti photocredits). **b** Skeleton of the colony at this stage. **c** Young colony at 2 polyp-stage. (after Lacaze Duthiers 1864). **d** Skeleton of the colony at this stage. **e** Skeleton of a young colony at 4 polyp-stage. **f** Skeleton of a 2–3-year-old colony: this “x profile” will form the central core in older colonies. **g** Thin section of an older colony axis: the central core is highlighted by the arrow



210 along the branches (135 basal sections and 62 internodal
211 and apical sections) were stained and examined to identify
212 the locations of polyps (i.e., cavity marks) and to estimate
213 their age. On thin sections, each annual growth ring is
214 made up of two seasonal bands (light and dark), with
215 crenulations in correspondence to the deep gastrodermal
216 channels (Fig. 1b, d). As these channels are absent on the
217 cavity mark surface, the lack of the crenulated layer along
218 growth rings indicates the presence of a polyp, and the
219 number of non-crenulated growth rings gives an estimate
220 of polyp age (Fig. 1d; Vielzeuf et al. 2008). A cavity mark
221 where the non-crenulated layer reaches the most external
222 growth ring (i.e., the most recent) indicates a polyp that
223 was still alive at the time of colony collection. When such a
224 marker was not present in the last growth ring (Fig. 1d), we
225 assumed that the polyp was already dead at the time of
226 collection (hereafter called “past polyp”). Polyps still alive
227 at the time of sampling were excluded from the calculation
228 of longevity and life span.

229 The mean number of living and past polyp marks were
230 divided according to the age of the colony at the level at
231 which the thin section was cut. The age of branches was
232 determined by applying the OMS method ($n = 162$).

233 As data were not normally distributed, a nonparametric
234 analysis (Mann–Whitney) was applied to test if polyp age
235 differs between females ($n = 82$) and males ($n = 93$), and
236 between shallow ($n = 168$) and deep ($n = 63$) populations.

237 The average width of polyp cavity marks (i.e., the linear
238 distance between the two edges of the depression), mea-
239 sured on the most evident cavities ($n = 114$), was used as a
240 proxy for polyp diameter. Polyp growth rates (mm y^{-1})
241 were then calculated as the ratio between cavity mark
242 width and polyp age.

243 The density of polyps was measured on 10 living
244 colonies maintained alive in aquaria at 17 ± 1 °C (sam-
245 pling details in Supplemental Materials). The number of
246 polyps on the three branch types (basal $n = 10$, internodal

247 $n = 10$ and apical $n = 10$) was counted under a dissecting
248 microscope. For accuracy, polyp counts were performed
249 twice, and the average value was used for the analysis.
250 The length (distance, in mm, between the branch base and
251 tip) and mean diameter (in mm, at the branch base and
252 tip) of each branch on the colony skeletons were mea-
253 sured with calipers and the branch surface (cm^2) was
254 calculated by approximating their shape to a truncated
255 cone. Polyp density (number $\times \text{cm}^{-2}$) was calculated by
256 dividing the polyp number by the area of each branch. In
257 order to account for autocorrelation of data within a
258 colony, polyp density in different branches of colonies
259 was analyzed using a linear mixed model, including the
260 branch types as a fixed effect and the colony as a random
261 effect (model $< - \text{lmer}(\text{Density} \sim \text{Branchtypes} + (1|\text{Col-}$
262 $\text{ony}))$, using the function ‘lmer’ in the R package ‘lme4’
263 (Bates et al. 2015). In order to assess the fit of the model,
264 we calculated the marginal and conditional R^2 , using the
265 function r.squared GLMM in the package MuMIn (Barton
266 2019). The marginal R^2 provides an estimate of the propor-
267 tion of total variance explained by the fixed factor alone,
268 while the conditional R^2 an estimate of that explained by both
269 the fixed and random factors (Nakagawa and Schielzeth
270 2013). We tested the effects of Branch Type in the linear
271 mixed model with a Type-III ANOVA (Table 1), using
272 Satterthwaite’s method (lmerTest package; Kuznetsova et al.
273 2017). The function ‘lsmeans’ in the R package ‘lsmeans’
274 (Lenth 2016) was used for post hoc comparisons among
275 Branch Type levels. Assumptions of linearity and homo-
276 geneity of variance were checked by means of Q–Q plots and
277 by plotting residuals versus fitted values.

Mortality table and budding rate

278
279 Based on the age of past polyps, a mortality table was
280 constructed (i.e., a life table based on the age of polyps at
281 death; Bergher 1990; Arrigoni et al. 2011; Table 2). In this

Table 1 (a) Type-III ANOVA of polyp density. (b) Post hoc comparisons among Branch Type levels

| (a) | | | | | | |
|----------------------------|----------|---------|--------|----------------|----------------|------------------|
| | Sum Sq | Mean Sq | Num DF | Den DF | <i>F</i> value | Pr (> <i>F</i>) |
| Branch Type | 325.91 | 162.96 | 2 | 18 | 10.344 | 0.001022 |
| (b) | | | | | | |
| Contrast | Estimate | SE | DF | <i>t</i> ratio | <i>p</i> value | |
| Apical-basal branches | 8.06 | 1.78 | 18 | 4.541 | 0.0007 | |
| Apical-internodal branches | 4.43 | 1.78 | 18 | 2.494 | 0.0560 | |
| Basal- internodal branches | − 3.63 | 1.78 | 18 | − 2.047 | 0.1298 | |



282 table, polyps were divided into yearly age classes, and the
283 number of dead (X_i) and survivors (S_i) during each age
284 interval reported.

285 Mortality values were used to construct a survival
286 transition matrix (Table 3), in which the nonzero entries in
287 the lower diagonal are the probabilities (σ_i) of polyp sur-
288 vival from one age class (i) to the next ($i + 1$). The data
289 presented in Tables 2 and 3 were used to develop a model
290 describing the polyp budding rate in a young, unbranched
291 colony; as this rate is most likely similar to that of a new
292 branch, this parameter will hereafter be referred to as
293 “branch budding rate.” Then, the polyp number at the
294 colony base was projected over a period of 50 years. A
295 detailed description of the model and calculations of bud-
296 ding rate variability are reported in the Supplemental
297 Materials.

298 Results

299 Skeleton formation and dynamics of polyp number

300 The early formation of the skeleton was described on the
301 basis of the observation of polyp cavity marks in 1–4-year-
302 old colonies. A few weeks after larval settlement, the new
303 whitish polyp starts to deposit sclerites in the coenosarc,
304 forming the first cavity of the primary polyp (L Bramanti
305 personal observations; Fig. 2a, b). After two months, when
306 the young colony has two polyps (Fig. 2c), two adjacent
307 cavities are visible in the skeleton (Fig. 2d). Four cavities
308 from a quartet of adjacent polyps were evident in 1-year-
309 old colony skeletons (Fig. 2e). During the first 4 years,
310 only the skeleton between adjacent cavities grows and form
311 an “x-shaped profile” (from a vertical point of view,
312 Fig. 2f), which becomes the butterfly-like structure
313 observed in the transversal sections of the central skeletal
314 core of > 4 years old colonies (arrow in Fig. 2g).

315 In branched colonies, older than 10 years, there was no
316 relationship between colony age and polyp number. How-
317 ever, a significant, correlation described by a power func-
318 tion was found between the number of polyps in a colony
319 and the number of its apical branches ($y = 23.87x^{0.91}$,
320 $R^2 = 0.62$, $p < 0.01$, $n = 548$; Fig. 3). This suggests that
321 the total number of polyps is linked to the number of
322 branches rather than to colony age.

323 Polyp age and distribution

324 A total of 197 transversal sections of *C. rubrum* skeletons
325 were examined and 355 polyp cavity marks identified (234
326 of past polyps and 121 of polyps that were still alive at the
327 time of colony collection). Living polyps were more
328 abundant in sections cut from the younger branches of a

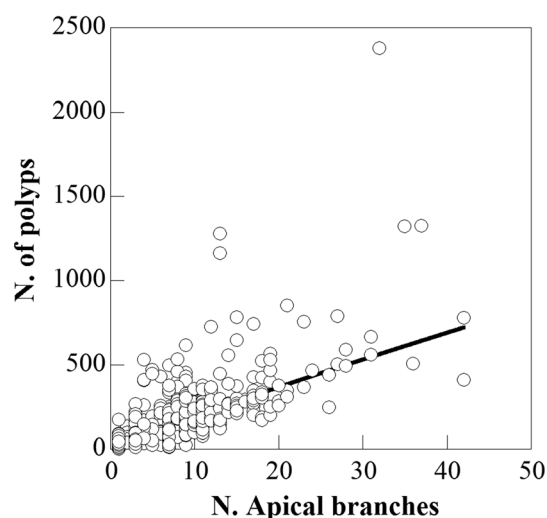


Fig. 3 Relationship between apical branch and polyp number: $y = 23.87x^{0.91}$, $R^2 = 0.62$, $p < 0.01$, $ES = 138$

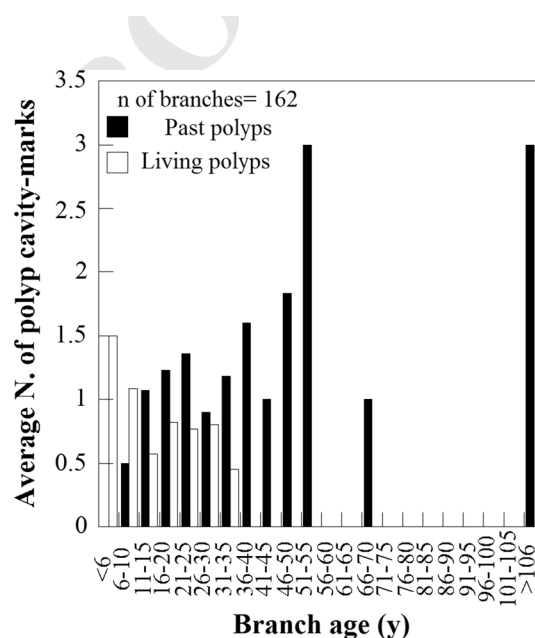


Fig. 4 Mean number of polyp cavity marks per colony branches of different age classes

colony (< 10 years), with their number decreasing with
branch age. Only past polyp markers were found on branch
sections older than 35 years (Fig. 4).

Despite the wide variability in polyp longevity, no polyp
(out of the 355 examined) was older than 12 years sug-
gesting that senescence is likely an important process in
regulating polyp dynamics within colonies. The median
age of past polyps and their maximum life span were 4 and
12 years, respectively ($n = 234$; Fig. 5).

As expected, living polyps were generally younger than
past ones, accounting for 45% of the < 1-year-old ones.

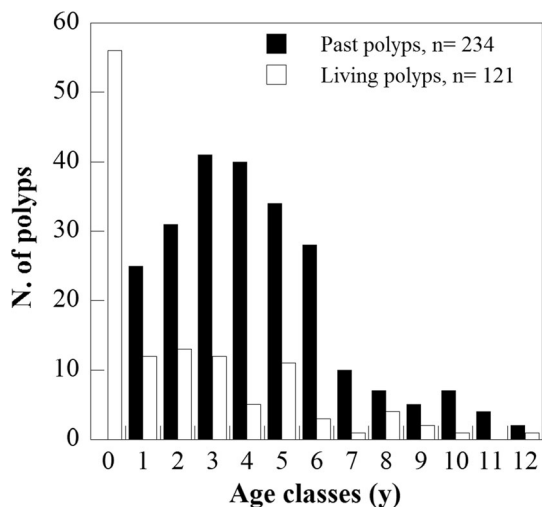


Fig. 5 Age distribution of living and past polyps

340 As < 1-year-old polyps do not form cavity marks in the
 341 growth ring layer, it is not possible to individuate these
 342 polyps on the thin sections, but they can be identified only
 343 if they were alive at the time of collection through the
 344 remains of their tissue.

345 There was no significant difference in longevity between
 346 polyps of female and male colonies (Mann–Whitney Test,
 347 $n = 82, n = 93, p > 0.05$) while polyps of deeper colonies
 348 were significantly older than those of shallow ones (5.5 vs.
 349 4 years, Median, Mann–Whitney Test: $n = 66, n = 168;$
 350 $p < 0.001$).

351 The median diameter of cavity marks was 1.0 mm (C.I.
 352 0.98–1.03 mm, $n = 114$), and it is reached within the first
 353 or the second year of polyp life.

354 The density of polyps varied significantly among dif-
 355 ferent branches (Table 1a and Fig. 6a). Post hoc tests
 356 indicated that polyp density at the apical branches
 357 (16.1 ± 1.7 polyps cm^{-2} , Mean \pm ES) was higher than at
 358 the basal branch (8.0 ± 1.2 polyps cm^{-2}). Likewise, there
 359 was a trend for polyp density on internodal branches to be

Fig. 6 a Polyp density in different branches of the colony. Bars = SE. **b** Polyp density versus age of basal, internodal and apical branches ($y = 28.3 - 11.7 \log(x), R^2 = 0.47, p < 0.05$)

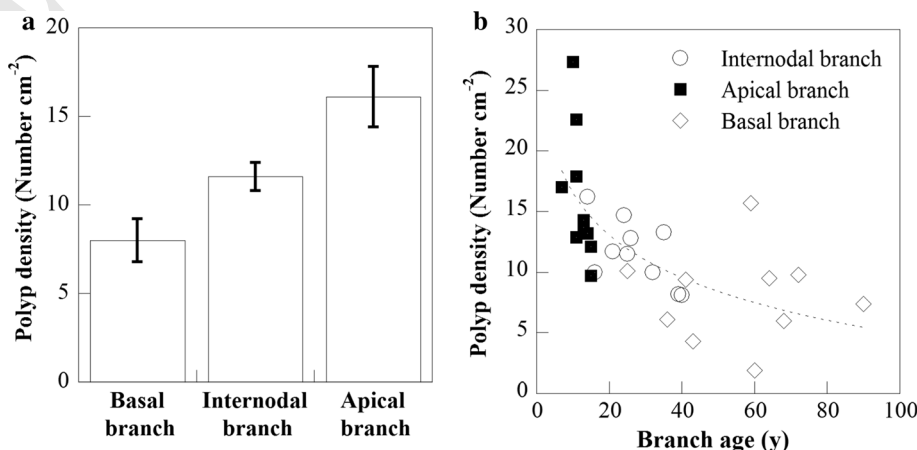


Table 2 Mortality table constructed from the age at death of 234 polyps

| Polyp age classes (<i>i</i>) | X_i | S_i | l_i |
|--------------------------------|-------|-------|-------|
| 1–2 | 25 | 234 | 1.00 |
| 2–3 | 31 | 209 | 0.89 |
| 3–4 | 41 | 178 | 0.76 |
| 4–5 | 40 | 137 | 0.59 |
| 5–6 | 34 | 97 | 0.41 |
| 6–7 | 28 | 63 | 0.27 |
| 7–8 | 10 | 35 | 0.15 |
| 8–9 | 7 | 25 | 0.11 |
| 9–10 | 5 | 18 | 0.08 |
| 10–11 | 7 | 13 | 0.06 |
| 11–12 | 4 | 6 | 0.03 |
| 12–13 | 2 | 2 | 0.01 |
| 13–14 | 0 | 0 | 0.00 |

X_i = number of polyps that died during each age interval; S_i = number of survivors at the beginning of each age interval; l_i = survival probability of class 1 polyps to age class (*i*) (number of survivors as a fraction of newborns)

higher than at the base of colonies, but differences were 360
 only marginally significant. There were no differences in 361
 polyp density between internodal and apical branches 362
 (Table 1b). The linear mixed model explained about 44% 363
 of the variation in the data (conditional $R^2 = 0.436$), of 364
 which around 40% was explained by the fixed factor (i.e., 365
 Branch type; marginal $R^2 = 0.402$). 366

Polyp density decreased with the age of branches and 367
 higher values were found at some tips (Fig. 6b). 368

Mortality and Budding rate 369

Mortality regularly increased with polyp age and 59% of 370
 polyps died before the age of 5 years (age classes 5–6). All 371

Table 3 Survival transition matrix of a *Corallium rubrum* polyp population. The diagonal represents the portion (σ_i) of polyps that raised by one class to the following each year

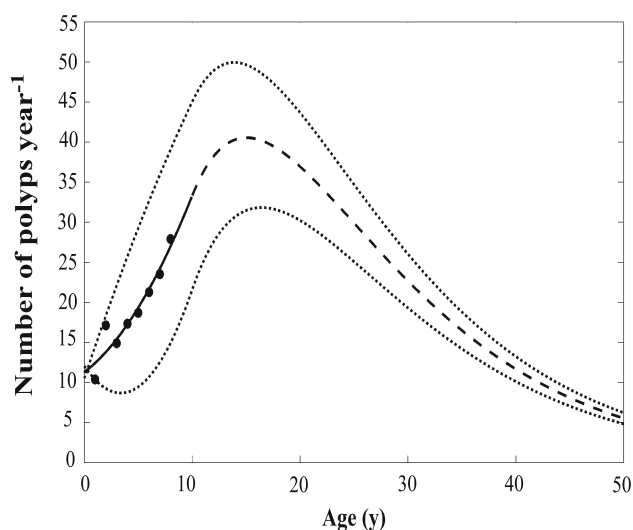
$$\begin{pmatrix} 0 & 0 & 0 & 0 & 0 & 0 & 0 & 0 & 0 & 0 & 0 & 0 \\ 0.89 & 0 & 0 & 0 & 0 & 0 & 0 & 0 & 0 & 0 & 0 & 0 \\ 0 & 0.85 & 0 & 0 & 0 & 0 & 0 & 0 & 0 & 0 & 0 & 0 \\ 0 & 0 & 0.77 & 0 & 0 & 0 & 0 & 0 & 0 & 0 & 0 & 0 \\ 0 & 0 & 0 & 0.71 & 0 & 0 & 0 & 0 & 0 & 0 & 0 & 0 \\ 0 & 0 & 0 & 0 & 0.65 & 0 & 0 & 0 & 0 & 0 & 0 & 0 \\ 0 & 0 & 0 & 0 & 0 & 0.56 & 0 & 0 & 0 & 0 & 0 & 0 \\ 0 & 0 & 0 & 0 & 0 & 0 & 0.71 & 0 & 0 & 0 & 0 & 0 \\ 0 & 0 & 0 & 0 & 0 & 0 & 0 & 0.72 & 0 & 0 & 0 & 0 \\ 0 & 0 & 0 & 0 & 0 & 0 & 0 & 0 & 0.72 & 0 & 0 & 0 \\ 0 & 0 & 0 & 0 & 0 & 0 & 0 & 0 & 0 & 0.46 & 0 & 0 \\ 0 & 0 & 0 & 0 & 0 & 0 & 0 & 0 & 0 & 0 & 0.33 & 0 \end{pmatrix}$$


Fig. 7 Branch budding rate over time. Continuous line: values of β_n (branch budding rate) for a young and unbranched colony of age ranging from 1 to 9 years (data from Bramanti et al. 2005 and Santangelo et al. 2007). Dashed line: estimated β_n from 10 to 50 years. The two dotted curves represent the variability of β_n

372 polyps of a new, annual cohort (age class) died within
373 12 years; thus the complete turnover of a colony could
374 occur several times during its life cycle (e.g., a colony
375 100 years old could renew its polyps about 8 times).

376 A mortality table was constructed using the age at death
377 of past polyps (Table 2). In this table, polyps were divided
378 into 13 yearly age classes, and the yearly number of dead
379 (X_i) and survivors (S_i) were reported. The polyp mortality
380 table was, then, used to compile a survival transition matrix
381 which describes the portion of polyps that, for each year,
382 passed from one age class to the following (Table 3). The
383 matrix was then applied to develop a dynamic population
384 model which fits the polyp budding rate of a young,
385 unramified colony (data from the literature in Supplemental

Materials) and projects this rate up to 50 years (during this
386 time the young colony became the basis of an older, larger
387 one; Fig. 7). According to the model, the yearly number of
388 polyps increases (up to 40 polyps year⁻¹) with the age of
389 branches and, after 15–16 years, it decreases reaching the
390 lowest value (< 10 polyps years⁻¹) at 50 years. The model
391 is based on average values and the variability around these
392 values was calculated as reported in Supplemental Mate-
393 rials and represented by dotted lines in Fig. 7. 394

Discussion 395

Understanding the mechanisms underpinning the organi-
396 zation of polyps by an a posteriori demographic approach
397 could shed some new light on the growth of long-lived,
398 branched gorgonians. In *Corallium rubrum*, the colony
399 shape may be described by a blend between the bifurcation
400 model, in which “a single branch divides in two sisters
401 branches” (Brazeau and Lasker 1992) and the mother-
402 daughter branching model, in which “colonies branching
403 subapically, generating hierarchical mother-daughter rela-
404 tionships among branches” (Lasker et al. 2003; Sánchez
405 et al. 2004; among others). Simulations of the modular
406 growth of *C. rubrum* colonies have been developed on the
407 basis of simple stochastic rules and results suggested that
408 the morphology can result two conflicting processes,
409 branching and growth, priority of which is regulated by
410 environmental factors (Kahramanoğullari et al. 2019). 411

In the Mediterranean red coral, the overall number of
412 polyps is correlated with colony age during the first years
413 of life (Bramanti et al. 2005), while in the older colonies,
414 such as those examined here, this correlation is lost. In
415 these larger colonies, the number of polyps is a function of
416 the total number of apical branches that, despite the wide
417 variability in their size, are characterized by higher polyp
418 density. As the first ramification starts around 10 years
419 (Benedetti et al. 2016), the lack of a correlation between
420 polyp number and colony age in > 10 years old colonies is
421 likely the result of a large variation in the branching
422 process. 423

While the reproductive cycle of *C. rubrum* is well
424 known (Vighi 1972; Santangelo et al. 2003), the mecha-
425 nisms regulating the production of new polyps are still
426 poorly understood. The highly variable colony morphology
427 recorded in several octocorals, often considered as a con-
428 sequence of large variability in hydro-mechanical forces
429 (Patterson 1980; Chindapol et al. 2013; among others),
430 could be driven by polyp density and distribution. Perrin
431 et al. (2015) suggested that the direction of growth of new
432 branches in *C. rubrum* could be influenced by the position
433 of the polyp with respect to the tip: “...radially distributed
434 polyps could favor a uni-directional vertical growth, while
435

436 polyps located at the very tip of the branch could favor the
437 emergence of a ramification.” Occasionally, some polyps
438 can drive the growth of further secondary branches starting
439 from the base or well below the colony tips, probably by
440 increasing the production of sclerites at their bases (Perrin
441 et al. 2015; Benedetti et al. 2016).

442 A first attempt to model the evolution over time of polyp
443 number in a *C. rubrum* colony was recently made by Galli
444 et al. (2016), who assumed that new polyps are produced
445 by the older ones via a budding process that depends on the
446 number of polyps at budding time. However, differently
447 from scleractinians (e.g., Richmond 1997; Gateño and
448 Rinkevich 2003) and some octocorals (Lan da Silveira and
449 Van't Hof 1977), no budding in already existing polyps has
450 ever been documented in *C. rubrum*. The only description
451 of new polyp formation in colonies of this species dates
452 back to about 150 years ago, when the French naturalist,
453 Henry Lacaze Duthiers, described the “blastogenesis of a
454 polyp” as a “small whitish tumor” appearing on a point on
455 the colony surface (Lacaze Duthiers 1864). The lack of
456 polyp budding in the Mediterranean red coral has been
457 further confirmed by other researchers (S Rossi and G
458 Tsounis, pers. comm.). In conclusion the formation of new
459 polyps likely occurs on some points of the gastrodermal
460 channels embedded in the coenenchyma, following
461 modalities that are still unknown.

462 An analysis of the polyp distribution along colony
463 branches of different ages may provide a proxy for the
464 local budding rate of polyps. We found a significantly
465 higher density of polyps at the tips that together with its
466 decrease with increasing age suggests a higher rate of
467 production of new polyps in the younger parts of the col-
468 ony. Such observation is supported by the faster growth
469 rates in young colonies (Bramanti et al. 2005; 2007) and at
470 the tips (Benedetti et al. 2016; Lartaud et al. 2016). The
471 higher polyp density found at some tips, indicating faster
472 growth in some branches, could lead to directional and
473 asymmetrical colony growth.

474 At the base of branched colonies, polyp density and
475 diameter growth rates are lower and vertical growth stops
476 (Bramanti et al. 2014; Benedetti et al. 2016). The small
477 number of polyps found in this portion of the colony could
478 be explained by the limited plankton supply due to the
479 reduced current and the trophic shadow cast by higher rank
480 branches (Kim and Lasker 1997). We should then expect
481 that the sparse polyps found at the colony base may either
482 change their tentacles in response to a lower food supply
483 (Abel 1970; Lopez-Gonzalez et al. 2018) or shift from a
484 trophic to a cleaning/sweeping function.

485 Little is known about the life cycle of coral polyps. The
486 literature data are highly variable, spanning between the
487 observation made by Beklemishev (1969) who described
488 the polyps of colonial anthozoans as “short-lived,” and the

489 reports of Wood-Jones (1907) who believed that coral
490 polyps were theoretically immortal. In a more recent study
491 on scleractinian polyps, Darke and Barnes (1993) estimated
492 a mean polyp life expectancy of 5 years and a maximum
493 life span of 8 years. Moreover, they found a significant
494 difference in polyp longevity between colonies collected
495 on reefs characterized by different “bumpiness” (i.e.,
496 lenticular growth surface; Darke and Barnes 1993). To
497 date, measures of polyp life span in gorgonian corals are
498 rare. In the Mediterranean red coral, Vielzeuf et al. (2008)
499 report that “...a polyp appears, fulfills its functions, and
500 then disappears after 6–8 years of activity.” Using the
501 method described in the foregoing, we determined the age
502 distribution of polyps in *C. rubrum* colonies collected from
503 different geographic areas and depths. According to our
504 results, *C. rubrum* polyps reach their maximum size in the
505 first two years of life and have an average life span of
506 4 years, with no difference between females and males,
507 suggesting that the different time needed for female and
508 male gonad maturation (two and one year respectively;
509 Vighi 1972) does not influence polyp life span. Fifty-nine
510 percent of new polyps died before 5 years and their max-
511 imum life span was 12 years. A 100-year-old colony
512 should then pass through approximately 8 generations of
513 polyps: such polyp renewal could be a key factor in the
514 longevity of this species. In all colonies collected in the
515 different sampling areas, no polyp lived more than
516 12 years, polyp density decreased with branch age and
517 mortality increased with polyp age: these findings clearly
518 suggest the relevance of polyp senescence in determining
519 colony growth and longevity. However, this does not
520 exclude local, partial mortality due to predation (Priori
521 et al. 2015).

522 Our data indicate a significantly greater polyp age in
523 colonies collected in deeper (50–130 m depth) than shall-
524 lower areas (30–35 m depth). This difference is likely due
525 to the higher mean colony age found in deeper populations
526 (Tsounis et al. 2006a; Priori et al. 2013; Bramanti et al.
527 2014; Benedetti et al. 2016). As observed in several marine
528 modular organisms (Sánchez et al. 2004 and references
529 herein), the polyp budding rate in *C. rubrum* decreases with
530 branch age. Given that colony growth rate and polyp pro-
531 duction are higher during the first years of colony life
532 (Bramanti et al. 2005, 2014), it was expected that polyp
533 production would be faster in younger and less branched
534 colonies with respect to older ones.

535 Using the mortality table of polyps, a transition matrix
536 and a dynamic population model were set out to represent
537 the branch budding rate of polyps over a life span of
538 50 years. In a young, unbranched colony, the branch bud-
539 ding rate increases up to 15 years of life, to decrease in the
540 following period, when the formerly young colony
541 becomes the basis of an older, branched one. Such bell-

542 shaped trend is consistent with the reduction of polyp
543 density observed in the older parts of a colony, likely due
544 to senescence.

545 The demographic model proposed in this paper
546 describes the modular growth of young, unbranched *C.*
547 *rubrum* colonies. Our findings represent a first step toward
548 the development of advanced polyp dynamic models aimed
549 at representing the complex growth of older, ramified
550 colonies, in which also the second factor of modularity (*i.e.*
551 the branching process) and the variability of the growth
552 process, should be included.

553 **Acknowledgements** We would like to thank A. Malasoma and A.
554 Bernardeschi (TS Lab & Geoservices snc of Pisa) for their help
555 in preparing the red coral thin sections. We also wish to thank G. Galli
556 (Plymouth Marine Laboratory and Istituto Nazionale di Oceanografia
557 e Geofisica Sperimentale, Trieste) for his intriguing questions on
558 polyp life cycle, D. Vielzeuf (CINaM - Centre Interdisciplinaire de
559 Nanoscience de Marseille) for his useful suggestions on the manu-
560 script, and A. Cafazzo for his revision of the English text. This work
561 is part of the PhD Thesis of M.C. Benedetti, which has been funded
562 by Enzo Liverino s.r.l., Chii Lih Coral Co Ltd of Taiwan and the
563 University of Pisa.

564 References

- 565 Abel EF (1970) Über den Tentakelapparat der Edelkoralle (*Corallium*
566 *rubrum* L.) und seine Funktion beim Beutefangverhalten.
567 *Oecologia* 4:133–142
- 568 Arrigoni M, Manfredi P, Panigada S, Bramanti L, Santangelo G
569 (2011) Life-history tables of the Mediterranean fin whale from
570 stranding data. *Mar Ecol* 32:1–9
- 571 Barham E, Davies IE (1968) Gorgonian and water motion studies in
572 the Gulf of California. *Underwater Naturalist* 5:24–28
- 573 Barton K (2019) Package ‘MuMIn’. R package version, 1.43.15.
574 <https://CRAN.R-project.org/package=MuMIn>
- 575 Bates D, Maechler M, Bolker B, Walker S, Christensen RHB,
576 Singmann H, Dai B, Grothendieck G, Green P (2015) Package
577 ‘lme4’. *Convergence*, 12
- 578 Beklemishev WN (1969) Principles of comparative anatomy of
579 invertebrates. Oliver & Boyd, Edinburgh
- 580 Benedetti MC, Priori C, Erra F, Santangelo G (2016) Growth patterns
581 in mesophotic octocorals: timing the branching process in the
582 highly-valuable Mediterranean *Corallium rubrum*. *Estuar Coast*
583 *Shelf Sci* 171:106–110
- 584 Bergher J (1990) Persistence of different-sized populations: an
585 empirical assessment of rapid extinction in bighorn sheep.
586 *Conservation Biology* 4:91–98
- 587 Bramanti L, Magagnini G, De Maio L, Santangelo G (2005)
588 Recruitment, early survival and growth of the Mediterranean
589 red coral *Corallium rubrum* (L 1758), a 4-year study. *J Exp Mar*
590 *Bio Ecol* 314:69–78
- 591 Bramanti L, Rossi S, Tsounis G, Gili JM, Santangelo G (2007)
592 Settlement and early survival of red coral on artificial substrates
593 in different geographic areas: some clues for demography and
594 restoration. *Hydrobiologia* 580:219–224
- 595 Bramanti L, Iannelli M, Santangelo G (2009) Mathematical mod-
596 elling for conservation and management of gorgonians corals:
597 youngs and olds, could they coexist? *Ecol Model*
598 220:2851–2856

- 599 Bramanti L, Vielmini I, Rossi S, Tsounis G, Iannelli M, Cattaneo-
600 Vietti R, Priori C, Santangelo G (2014) Demographic parameters
601 of two populations of red coral (*Corallium rubrum* L. 1758) in
602 the North Western Mediterranean. *Mar Biol* 161:1015–1026
- 603 Bramanti L, Benedetti MC, Cupido R, Cocito S, Priori C, Erra F,
604 Iannelli M, Santangelo G (2017) Demography of animal forests:
605 the example of mediterranean gorgonians. In: Rossi S, Bramanti
606 L, Gori A, Orejas C (eds) Marine animal forests. Springer
607 international publisher, pp 1–20
- 608 Brazeau DA, Lasker HR (1992) Growth rates and growth strategy in a
609 clonal marine invertebrate, the Caribbean octocoral *Briareum*
610 *asbestinum*. *Biol Bull* 183:269–277
- 611 Burlando B, Cattaneo-Vietti R, Parodi R, Scardi M (1991) Emerging
612 fractal properties in gorgonian growth forms (Cnidaria: octoco-
613 rallia). *Growth Dev Aging* 55:161–168
- 614 Caswell H (2001) Matrix population models: construction, analysis
615 and interpretation, 2nd edn. Sinauer Associates, Sunderland,
616 Massachusetts
- 617 Cau A, Bramanti L, Cannas R, Follesa MC, Angiolillo M, Canese SP,
618 Bo M, Cucco D, Guizien K (2016) Habitat constraints and self-
619 thinning shape Mediterranean red coral deep population struc-
620 ture: Implications for conservation practice. *Sci Rep* 6
- 621 Chindapol N, Kaandorp JA, Cronemberger C, Mass T, Genin A
622 (2013) Modelling growth and form of the scleractinian coral
623 *Pocillopora verrucosa* and the influence of hydrodynamics.
624 *PLoS Comput Biol* 9:e1002849
- 625 Cicogna F, Cattaneo-Vietti R (1993) Red coral in the Mediterranean
626 Sea, art, history and science. Ministero Risorse Agricole,
627 Alimentari e Forestali, Roma
- 628 Coma R, Ribes M, Gili JM, Hughes RN (2001) The ultimate
629 opportunists: consumers of seston. *Mar Ecol Prog Ser*
630 219:305–308
- 631 Costantini F, Rossi S, Pintus E, Cerrano C, Gili JM, Abbiati M (2011)
632 Low connectivity and declining genetic variability along a depth
633 gradient in *Corallium rubrum* populations. *Coral reefs*
634 30:991–1003
- 635 Darke WM, Barnes DJ (1993) Growth trajectories of corallites and
636 ages of polyps in massive colonies of reef-building corals of the
637 genus *Porites*. *Mar Biol* 117:321–326
- 638 Fujiwara M, Caswell H (2001) Demography of endangered North
639 Atlantic right whale. *Nature* 414:537–541
- 640 Galli G, Bramanti L, Priori C, Rossi S, Santangelo G, Tsounis G,
641 Solidoro C (2016) Modelling red coral (*Corallium rubrum*)
642 growth in response to temperature and nutrition. *Ecol Modell*
643 337:137–148
- 644 Gallmetzer I, Haselmai A, Velimirov B (2010) Slow growth and early
645 sexual maturity: bane and boon for the red coral *Corallium*
646 *rubrum*. *Estuar Coast Shelf Sci* 90:1–10
- 647 Garrabou J, Sala E, Linares C, Ledoux JB, Montero-Serra I, Dominici
648 JM, Kipson S, Teixidò N, Cebrian E, Kersting DK, Harmelin JG
649 (2017) Re-shifting the ecological baseline for the overexploited
650 Mediterranean red coral. *Sci Rep* 7:42404
- 651 Gateño D, Rinkevich B (2003) Coral polyp budding is probably
652 promoted by a canalized ratio of two morphometric fields. *Mar*
653 *Biol* 142:971–973
- 654 General Fisheries Commission for the Mediterranean Scientific
655 Advisory Committee, GFCM-FAO (2011) Report of the second
656 transversal workshop on red coral. Ajaccio, Corsica, France, 5-7
657 October 2011
- 658 Goffredo S, Lasker HR (2006) Modular growth of a gorgonian coral
659 can generate predictable patterns of colony growth. *Estuar Coast*
660 *Shelf Sci* 336:221–229
- 661 Gori A, Rossi S, Linares S, Berganzo E, Orejas C, Dale MRT, Gili JM
662 (2011) Size and spatial structure in deep versus shallow
663 population of the Mediterranean gorgonian *Eunicella singularis*

- 664 (Cap de Creus, northwestern Mediterranean Sea). *Mar Biol*
665 158:1721–1732
- 666 Grigg RW (1972) Orientation and growth form of sea fans. *Limnol*
667 *Oceanogr* 17:185–192
- 668 Grillo MC, Goldberg WM, Allemand D (1993) Skeleton and sclerite
669 formation in the precious red coral, *Corallium rubrum*. *Mar Biol*
670 117:119–128
- 671 Guizien K, Ghisalberti M (2017) Living in the canopy of the animal
672 forest: physical and biogeochemical aspects. In: Rossi S,
673 Bramanti L, Gori A, Orejas C (eds) *Marine animal forests*.
674 Springer international publisher, pp 507–528
- 675 Hageman SJ (2003) Complexity generated by iteration of hierarchical
676 modules in Bryozoa. *Integr Comp Biol* 43:87–98
- 677 Hageman SJ, Bock PE, Bone Y, McGowan B (1998) Bryozoan
678 growth habits: classification and analysis. *J Paleontol*
679 72:418–436
- 680 Harper JL (1977) *Population biology of plants*. Academic press,
681 London
- 682 Harper JL, Bell AD (1979) The population dynamics of growth form
683 in organisms with modular construction. In: Anderson RM,
684 Turner BD, Taylor LP (eds) *population dynamics*. Blackwell
685 Science Publisher, London, pp 29–52
- 686 Kaandorp JA, Küler JE (2001) The algorithmic beauty of seaweeds,
687 sponges and corals. Springer, Berlin
- 688 Kahramanoğullari O, Bramanti L, Benedetti MC (2019) Stochastic
689 Mechanisms of Growth and Branching in the Mediterranean
690 Coral Colonies. International Conference on Theory and Practice
691 of Natural Computing. Springer, Cham, pp 57–69
- 692 Kim K, Lasker HR (1997) Flow-mediated resource competition in the
693 suspension feeding gorgonian *Plexaura homomalla* (Esper).
694 *J Exp Mar Biol Ecol* 215:49–64
- 695 Kim K, Lasker HR (1998) Allometry of resource capture in colonial
696 cnidarians and constraints on modular growth. *Funct Ecol*
697 12:646–654
- 698 Knittweis L, Aguilar R, Alvarez H, Borg JA, Evans J, Garcia S,
699 Schembri PJ (2016) New depth record of the precious red coral
700 *Corallium rubrum* for the Mediterranean. *Rapport de la Com-*
701 *mission internationale de la Mer Méditerranée* 41
- 702 Kuznetsova A, Brockhoff PB, Christensen RHB (2017) LmerTest
703 package: Tests in linear mixed effects models. *J. Stat. Softw.* 82:
704 1–26. <https://doi.org/10.18637/jss.v082.i13>
- 705 Lacaze Duthiers H (1864) *Histoire naturelle du corail*, Paris
- 706 Lan da Silveira F, Van't Hof T (1977) Regeneration in *Plexaura*.
707 *Bijdragen tot de dierkunde* 47:98–108
- 708 Lasker HR, Boller ML, Castanaro J, Sanchez JA (2003) Determinate
709 growth and modularity in a gorgonian octocoral. *Biol Bull*
710 205:319–330
- 711 Lartaud F, Galli G, Raza A, Priori C, Benedetti MC, Cau A,
712 Santangelo G, Iannelli M, Solidoro C, Bramanti L (2016)
713 Growth patterns in long-lived animals. In: Rossi S, Bramanti L,
714 Gori A, Orejas C (eds) *Marine animal forests*. Springer
715 international publisher, pp 595–626
- 716 Lenth RV (2016) Least-squares means: the R package lsmeans.
717 *Journal of statistical software* 69:1–33
- 718 Lopez-Gonzalez P, Bramanti L, Escribano-Álvarez P, Benedetti MC,
719 Martínez-Baraldés I, Megina C (2018) Thread-like tentacles in
720 the Mediterranean corals *Paramuricea clavata* and *Corallium*
721 *rubrum*. *Mediterr. Mar, Scie*
- 722 Marschal C, Garrabou J, Harmelin JG, Pichon M (2004) A new
723 method for measuring growth and age in the precious red coral
724 *Corallium rubrum* (L.). *Coral Reefs* 23:423–432
- 725 Matsumoto AK (2004) Heterogeneous and compensatory growth in
726 *Melithaea flabellifera* (Octocorallia: melithaeidae) in Japan.
727 *Hydrobiologia* 530:389–397
- 728 Merks RMH, Hoekstra AG, Kaandora JA, Sloot PMA (2004) Polyp
729 oriented modelling of coral growth. *J Theor Biol* 228:559–576
- Nakagawa S, Schielzeth H (2013) A general and simple method for
730 obtaining R^2 from generalized linear mixed-effects models.
731 *Methods Ecol. Evol.* 4:133–142
- Patterson MR (1980) Hydromechanical adaptations in *Alcyonium*
732 *sidereum* (Octocorallia). In: Schneck DJ (ed) *Biofluid Mechanics*
733 2. Springer, Boston MA, pp 183–201
- Pedoni C, Follesa MC, Cannas R, Matta G, Pesci P, Cau A (2009)
734 Preliminary data on red coral (*Corallium rubrum*) population of
735 Sardinian Sea (Western Mediterranean). In: UNEP-MAP-RAC/
736 SPA, Proceedings of the 1st symposium on conservation of the
737 coralligenous bio-concretions. Pergent-Martini C, Bricchet (eds)
738 RAC/SPA publ. Tunis
- Perrin J, Vielzeuf D, Ricolleau A, Dallaporta H, Valton S, Floquet N
739 (2015) Block-by-block and layer-by-layer growth modes in coral
740 skeletons. *Am Mineral* 100:681–695
- Picciano M, Ferrier-Pagès C (2007) Ingestion of pico-and nanoplank-
741 ton by the Mediterranean red coral *Corallium rubrum*. *Mar Biol*
742 150:773–782
- Priori C, Mastascusa V, Erra F, Angiolillo M, Canese S, Santangelo G
743 (2013) Demography of deep-dwelling red coral populations: age
744 and reproductive structure of a highly valued marine species.
745 *Estuar Coast Shelf Sci* 118:43–49
- Priori C, Erra F, Angiolillo M, Santangelo G (2015) Effects of
746 gastropod predation on the reproductive output of an overex-
747 ploited deep octocoral. *Coral Reefs* 34:59–63
- Richmond RH (1997) Reproduction and recruitment in corals: critical
748 links in the persistence of reefs. In: Birkeland C (ed) *Life and*
749 *death of coral reefs*. Chapman & Hall, New York, pp 175–197
- Rosen BR (1986) Modular growth and form of corals: a matter of
750 metamers? *Philos Trans R Soc Lond B Biol Sci* 313:115–142
- Rossi S, Rizzo L, Duchêne J (2019) Polyp expansion of passive
751 suspension feeders: a red coral case study. *PeerJ*
752 Preprints 7:e27490v1
- Rowley SJ, Pochon X, Watling L (2015) Environmental influences on
753 the Indo-Pacific octocoral *Isis hippuris* Linnaeus 1758 (Alcy-
754 onacea: isididae): genetic fixation or phenotypic plasticity? *PeerJ*
755 3:e1128
- Russo AR (1985) Ecological observations on the gorgonian sea fan
756 *Eunicella cavolinii* in the Bay of Naples. *Mar Ecol Prog Ser*
757 24:155–159
- Sánchez JA, Lasker HR (2003) Patterns of morphological integration
758 in marine modular organisms: supra-module organization in
759 branching octocoral colonies. *Proc R Soc Lond B Biol Sci*
760 270:2039–2044
- Sánchez JA, Lasker HR, Nepomuceno EG, Sánchez JD, Woldenberg
761 MJ (2004) Branching and self-organization in marine modular
762 colonial organisms: a model. *Am. Nat.* 163:24–39
- Sánchez JA, Aguilar C, Dorado D, Manrique N (2007) Phenotypic
763 plasticity and morphological integration in a marine modular
764 invertebrate. *BMC Evolutionary Biology* 7:122
- Santangelo G, Abbiati M (2001) Red coral: conservation and
765 management of an over-exploited Mediterranean species. *Aquat*
766 *Conserv* 11:253–259
- Santangelo G, Carletti E, Maggi E, Bramanti L (2003) Reproduction
767 and population sexual structure of the overexploited Mediter-
768 ranean red coral *Corallium rubrum*. *Mar Ecol Prog Ser*
769 248:99–108
- Santangelo G, Bramanti L, Iannelli M (2007) Population dynamics
770 and conservation biology of the over-exploited Mediterranean
771 red coral. *J Theor Biol* 244:416–423
- Santangelo G, Cupido R, Cocito S, Bramanti L, Priori C, Erra F,
772 Iannelli M (2015) Effects of increased mortality on gorgonian
773 corals (Cnidaria, Octocorallia): different demographic features
774 may lead affected populations to unexpected recovery and new
775 equilibrium points. *Hydrobiologia* 759:171–187

- 795 Shaish L, Abelson A, Rinkevich B (2006) Branch to colony trajectory
796 in a modular organism: pattern formation in the Indo-Pacific
797 coral *Stylophora pistillata*. Dev Dyn 235:2111–2121
- 798 Shaish L, Abelson A, Rinkevich B (2007) How Plastic Can
799 Phenotypic Plasticity Be? The Branching Coral *Stylophora*
800 *pistillata* as a Model System. PLoS ONE 2:e644
- 801 Sherwood OA (2006) Deep-sea octocorals: dating methods, stable iso-
802 topic composition, and proxy records of the slopewaters off
803 Nova Scotia. PhD Thesis, Dalhousie University Halifax, Nova
804 Scotia
- 805 Thresher RE, MacRae CM, Wilson NC, Fallon S (2009) Feasibility of
806 age determination of deep-water bamboo corals (Gorgonacea;
807 Isididae) from annual cycles in skeletal composition. Deep Sea
808 Res Part 1 Oceanogr Res Pap 56: 442–449
- 809 Tsounis G, Rossi S, Gili JM, Arntz W (2006a) a) Population structure
810 of an exploited benthic cnidarian: the case study of red coral
811 (*Corallium rubrum* L.). Mar Biol 149:1059–1070
- 812 Tsounis G, Rossi S, Laudien J, Bramanti L, Fernandez N, Gili JM,
813 Arntz W (2006b) b) Diet and seasonal prey capture rates in the
Mediterranean red coral (*Corallium rubrum* L.). Mar Biol 149:313–325
- Tsounis G, Rossi S, Grigg R, Santangelo G, Bramanti L, Gili JM
(2010) The exploitation and conservation of precious corals.
Oceanography And Marine Biology; An Annual Review
48:161–212
- Vielzeuf D, Garrabou J, Baronnet A, Grauby O, Marschal C (2008)
Nano to macroscale biomineral architecture of red coral
(*Corallium rubrum*). Am Mineral 93:1799–1815
- Vighi M (1972) Etude sur la reproduction du *Corallium rubrum*. Vie
Milieu 23:21–32
- Williams GS (1975) The strawberry coral model. In: Sex and
evolution. Princeton, NJ: Princeton University Press
- Wood-Jones F (1907) On the growth forms and supposed species in
corals. Proceedings of the Zoological Society of London
77:518–556
- Publisher's Note** Springer Nature remains neutral with regard to
jurisdictional claims in published maps and institutional affiliations.